Impacts of ACCVD grown CNTs on hardness, compression and fracture behaviors of Stellite-6/CNTs nanocomposites

GHUZANFAR SAEED[a,*], FAZAL AHMAD KHALID[a], TARIQ SAEED CHANI[b], MUHAMMAD UMER FAROOQ[a], IRFAN H. ABIDI[a], TAHIR SATTAR[a]

[a]Faculty of Materials Science and Engineering, GIK Institute of Engineering Sciences and Technology, Topi (23640), KPK, Pakistan
[b]Chemistry Department, Faculty of Science, King Abdulaziz University, Jeddah 21589, Saudi Arabia

ACCVD grown CNTs via various ACCVD reaction times were used for the fabrication of Stellite-6/CNTs nanocomposites via powder metallurgy technique. Varied wt. % of CNTs (0.5, 1, 1.5 and 2) was used for nanocomposites development. Effects of varied CNTs wt. % on hardness, compression and fracture behaviors of Stellite-6/CNTs nanocomposites were the main investigating aspects of this study. Hardness behaviors of nanocomposites increased up to a critical wt. % of CNTs, after that there were deterioration in these values. There were some healthy impacts of CNTs on compression behaviors of nanocomposites and these enhanced in noticeable values up to a critical wt. % of CNTs. Varied higher wt. % of CNTs had not any influence on the fracture behavior of nanocomposites and it remain unchanged.

1. Introduction

Since the discovery of carbon nanotubes in 1991 [1], carbon nanotubes (CNTs) have provided opportunities to create new materials and devices for a variety of applications because of their remarkable physical, mechanical, chemical and electronic properties [2-4]. Addition of carbon nanotubes in composite matrix material as a reinforcement has led to the development of nanocomposites with superior mechanical properties as compared to the conventional composite materials [5-6]. There are three well-known techniques described to synthesize carbon nanotubes [7-9] that is electric arc, laser ablation and chemical vapor deposition. Among these techniques, CVD is considered better because of its simplicity in operation, high yield of CNTs, low operational cost and low temperature reaction [10-12].

The chemical vapor deposition process provides an opportunity to use carbon precursor in all three matter forms e.g. liquid, solid & gaseous forms for the growth of CNTs [13]. Previous work [14] reported synthesis of high quality SWCNTs using liquid precursor (methanol and ethanol) over Fe-Co catalysts supported on zeolite. Another study was also successful in the synthesis of high quality SWCNTs by alcoholic decomposition over catalyst powder using CVD method [15]. Synthesis of CNTs over conducting glass, nickel plates and porous alumina substrates is accomplished using Fe and Co acetates as

catalyst by ethanol decomposition [16]. Further investigation in the synthesis of high quality MWCNTs over pre-deposited Fe-catalyst thin film was carried out by ethanol decomposition [17]. The results of carbon nanotubes synthesized by ethanol decomposition showed better quality owing to OH⁻ radicals that are beneficial for the removal of amorphous carbon and other impurities [14, 18]. Fe, Co and Ni based nano-catalyst particles are beneficial in CNTs growth. As Stellite-6 is a Co based alloy and it was used for CNTs growth under different ACCVD reaction times. More details in our other study [19].

Stellite-6 alloy is applied for good mechanical and oxidation resistance which is important for wear and high temperature applications for bulk and hard coating alloy materials [20-21]. Possible applications of Stellite-6/CNTs nanocomposites may be for the development of hard alloy nano composite/coatings materials.

It was found that no systematic study has been conducted on the fabrication of Stellite-6/CNTs nanocomposites via powder metallurgy technique. CNTs used as reinforcing agents as described before were grown via ACCVD process at FMSE/GIKI laboratories. There were two main objectives of this study e.g. to investigate the strengthening behaviors of grown CNTs and to study the microstructural features of fractured nanocomposites surfaces.

2. Experimental details

For the fabrication of Stellite-6/CNTs nanocomposites, different wt. % of grown CNTs e.g. 0.5, 1, 1.5 and 2 were added as reinforcing agents in Stellite-6 matrix material. Nanocomposites were fabricated via powder metallurgy technique. Green compacts of Stellite-6/CNTs nanocomposites were sintered at 1250 °C for three hours and then were cooled to room temperature at cooling rate of 15 °C/min. Theses sintered plane and nanocomposites materials were further carried to studies the impact of varied wt. % of CNTs on hardness, compression and fractured behaviors of Stellite-6/CNTs nanocomposites. Macro-hardness of all samples was testified by Vickers hardness testing machine. Vickers load and dwelling time were 1 kg and 10 seconds respectively. To study the compressive strengthening behaviors of Stellite-6/CNTs nanocomposites, compression testing was performed by Jinan-te-universal testing machine with a cross-head of 0.1 mm/min. For micro studies of fractured surface, SEM (JEOL, JED-2300 station, Japan) analyses were performed.

3. Results and discussion

After fabrication of nanocomposites (with different wt. % of CNTs), macro-hardness was performed (Fig. 1). Hardness behaviors of nanocomposites were very interesting and encouraging (confirmed the grown CNTs strengthening behavior). Hardness of nanocomposites compacts increased within the increase of CNTs wt. % but this phenomena sustained up to a certain CNTs 1.5 wt. %. After this there was deterioration in hardness value at 2 wt. % of CNTs (Fig. 1).

There are three reasons to argue and justify the increased hardness behaviors of nanocomposites materials e.g. outstanding mechanical properties of CNTs, uniform dispersion of CNTs and hall pitch effects. Carbon nanotubes in today's nanocomposites world are the most demanding reinforcing agents due to their outstanding mechanical properties e.g. modulus of elasticity (1.28 TPa), fracture toughness (1240 J/g), tensile strength (14 GPa) and strain (12%) [22]. Higher modulus of elasticity values of grown CNTs may have helped in the improvement of nanocomposites hardness behaviors here.

Uniformly dispersed CNTs impart effective role to promote hardness behaviors of nanocomposites. As shown in Fig. 1 that hardness values for nanocomposites start to improve and it was maximum for Stellite-6 /1.5 wt. % CNTs nanocomposites. This is due to their uniform dispersion (Fig. 5) and these will provide reinforcing effects throughout the matrix material. As hardness values have deteriorated at 2 wt. % of CNTs (due to agglomeration phenomena). There had been reported lot of methods [23-26] to deal with CNTs agglomeration issues.
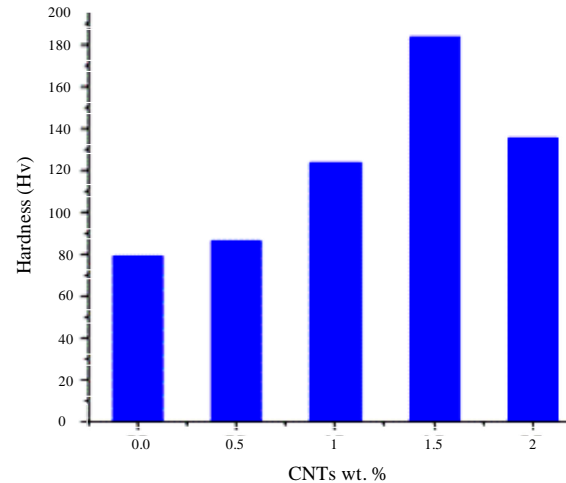

Fig. 1.Varied CNTs wt. % impact on hardness of Stellite-6/CNTs nanocomposites

Hardness of metallic nanocomposites is their resistance to plastic deformation. Plastic deformation is initiated by dislocations movement. To make materials more rigid and resistant to plastic deformation, restrict dislocations movement. Smaller the grain size of matrix, more resistance for dislocations to move. This relationship between hardness and grain size of matrix materials is well demonstrated by following Hall-Pitch equation.

$$Hv = Ho + \frac{k}{\sqrt{d}} \qquad (1)$$

Higher wt. % of CNTs had restrained the grain growth of Stellite-6/CNTs nanocomposites and this is proved by the improved hardness values (Fig. 1). From lower to higher (0.5-1.5) wt. % of CNTs, nano-reinforcing materials were dispersed uniformly and located individually on grain boundaries. These well dispersed CNTs had restricted grain growth of matrix material during sintering process. Grain growth was maximum restricted for Stellite-6/1.5 wt. % CNTs and it helped in nanocomposites hardness improvement according to Hall-Pitch relationship. As hardness values have deteriorated at 2 wt. % of CNTs (Fig. 1). The main reason for this deterioration is that CNTs were not uniform dispersed. Agglomerated CNTs located at grain boundaries could not well restrict grain growth during sintering process. Therefore, comparatively large grains size may evolve for Stellite-6/2 wt. % CNTs nanocomposites materials which do not prove effective to restrict dislocation movements.

Compression stress-strain behaviors of Stellite-6/CNTs nanocomposites were also testified and the results are shown in Fig. 2. In all these stress-strain curves three portions are very prominent: (a) maximum stress affording portion without plastic deformation, (b) where plastic deformation starts and (c) finally failure of nanocomposites materials. It can be seen that addition of varied higher wt. % of (1, 1.5 and 2) CNTs has noticeable impact on these three portions of stress-strain curves of nanocomposites.
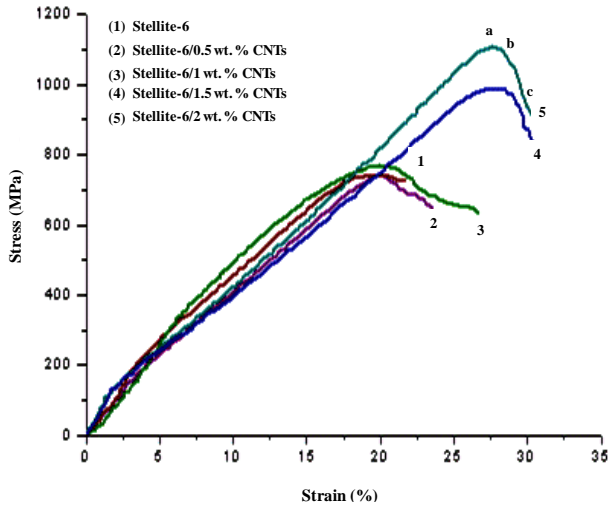
Fig. 2. Impact of varied wt. % of CNTs on compressive stress-strain behaviours of Stellite-6/CNTs nanocomposites

Compression properties like Ultimate Compression Strength (UCS) and compression strain failure % were quantify against varied wt. % of CNTs and results are graphically presented in Fig. 3 and Fig. 4 respectively. It is shown (Fig. 3) that Stellite-6/0.5 wt. % CNTs nanocomposites ultimate compression strength value is almost same as for plain Stellite compact. But ultimate compression strengths of nanocomposites containing 1, 1.5 and 2 wt % of CNTs are higher than plain Stellite-6 compact and Stellite-6/0.5 wt. % CNTs nanocomposites (Fig. 3). CNTs agglomeration (for maximum 2 wt. %) declining impact on compressive strengths of nanocomposites has not been notice here as strength of nanocomposites increase proportionally at maximum CNTs wt. % (Fig. 3).
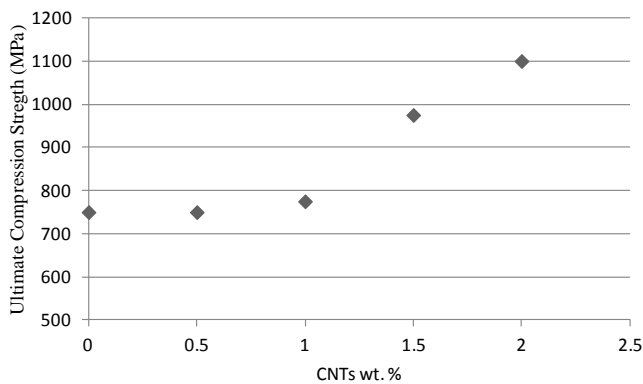

Fig. 3. Ultimate Compressive Strength (UCS) behaviours of Stellite-6/CNTs nanocomposites verses different varied wt. % of CNTs

There are number of possible mechanisms which support the increasing compression strength behaviors of Stellite-6/CNTs nanocomposites. (i) CNTs higher modulus of elastic values [22], (ii) generation of dislocations due to elastic modulus mismatch and co-efficient of thermal expansion mismatch between the nano-reinforcing particulates and matrix materials [27-28], (iii) Orowan strengthening mechanism [28], (iv) load transfer from matrix to reinforcing particulates [29] and (v) grain refinement caused by CNTs [30].
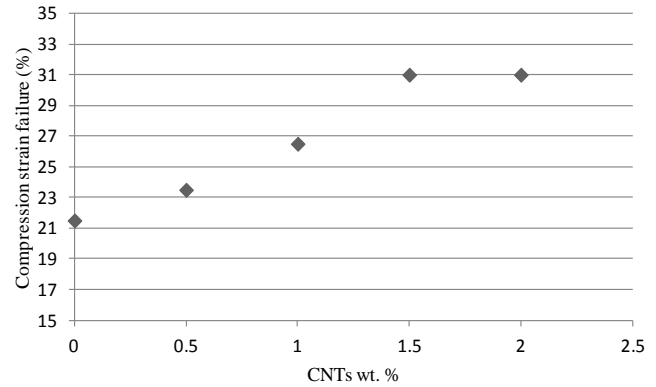

Fig. 4. Compression strain failures of Stellite/CNTs nanocomposites verses different varied wt. % of CNTs

The mismatch of elastic modulus and CTE between the Stellite-6 matrix (CTE of Stellite-6=0.19μm/m.K and shear modulus of Stellite-6=87 GPa) and CNTs particulates (CTE of CNT=0.20×10^{-5}μm/m.K and shear modulus of CNTs=1 GPa) promote dislocation generation in the vicinity of the matrix/particulates interfaces. Greater numbers of dislocations in nanocomposites yield higher level of internal stress to initiate plastic deformation. [29]. Possible generation of dislocations densities due to elastic modulus and CTE mismatch are respectively given by following equations 2 and 3 respectively.

$$\varrho EM = \frac{\gamma m}{b \Lambda} \qquad (2)$$

and

$$\varrho CTE = \frac{10 f \epsilon}{b(1-f)d} \qquad (3)$$

where, γ^m is the shear strain in the matrix, Λ presents local length scale of the deformation field, b is the Burgers vector, f is the volume fraction of particulates, ϵ is the misfit strain due to the different CTEs of Stellite-6 and CNTs, and d is the average diameter of particulates.

Yield strength of the nano-composites, $\Delta\sigma$, caused by mismatch of elastic modulus and CTE can be well estimated by following equation 4 [29].

$$\Delta\sigma = \sqrt{[(\Delta\sigma EM)2 + (\Delta\sigma CTE)2]} \qquad (4)$$

where, $\Delta\sigma_{EM}$ and $\Delta\sigma_{CTE}$ are the stress increment due to elastic modulus and coefficient of thermal expansion mismatch between the Stellite-6 matrix and CNTs particulates. These both parameters ($\Delta\sigma_{EM}$ & $\Delta\sigma_{CTE}$) can be calculated by followings Taylor relations respectively.

$$\Delta\sigma EM = \sqrt{3\alpha\mu m}b\sqrt{\varrho EM} \qquad (5)$$

and

$$\Delta\sigma CTE = \sqrt{3\beta\mu m}b\sqrt{\varrho CTE} \qquad (6)$$

where, α and β are the strengthening coefficients and μ_m is the shear modulus of the matrix.

The strength increase in the case of the nano-composites can also be attributed to the dislocation – impenetrable particulates interactions as described by the Orowan strengthening mechanism [28]. Miller and Humphreys demonstrated that this mechanism is effective when the size of reinforcing particulates is less than 1 μm. Due to the presence of CNTs particulates, geometrically necessary dislocation loops are formed around each nano-particulate after dislocation lines bow and bypass. These loops lead to promote high work hardening rate and help to strengthen the nano-composites materials. The contribution to yield strength by Orowan strengthening mechanism can be estimated by equation 7 [29].

$$\sigma Orowan = M\frac{0.4\mu m\ b}{\Pi\Lambda}\frac{\ln(\frac{b}{d})}{\sqrt{V\ stellite-6}} \qquad (7)$$

where, M is a strengthening coefficient, Λ is mean inter-particulate distance given by $\Lambda = d\ (\sqrt{\Pi}/4f-1)$.

During applied load (tensile or compressive) effective load transfer from matrix to reinforcement always dependent on the interfacial bonding between the reinforcement & the matrix and also on volume fraction of nano-particulates. According to the modified shear–lag model [29], the yield strength of a composite can be expressed by equation 8.

$$\sigma c = \sigma m\left(1+\frac{(L+t)A}{4L}\right)f + \sigma m(1-f) \qquad (8)$$

where, σc and σm are, respectively the yield stress of the composite and monolithic, L is the size of the particulate, t is the thickness of the particulate and A = L/t is the particulate aspect ratio.

The increase in the compressive strength of the nano-composites may also be attributed to the reduction in grain size [30] caused by CNTs particulates. Although all possible mechanisms have been discussed here in detail but as for as compression strength of Stellite-6/CNTs nanocomposites is concerned, three strengthening mechanisms are more dominating e.g. generation of dislocations process, Orowan relations and better load transfer between matrix and reinforcing particulates.

The compression strain failure % has increased gradually with the addition of CNTs and remains steady at maximum 2 wt. % of CNTs. The enhanced compression strain failure % of nanocomposites may be due to Orowan relations and generations of dislocations at reinforcing particulates/matrix interfaces. These both factors especially at higher wt. % of CNTs have helped nanocomposites materials to resist plastic deformation

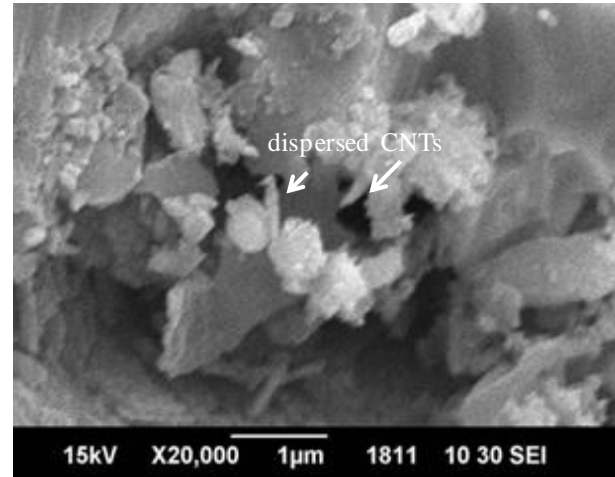maximum and to not deform catastrophically until their complete failure.

Fig. 5. Well dispersed CNTs in Stellite-6/1.5 wt. % CNTs nanocomposites

Stellite-6 is a brittle material and it is not characterized by fracture mode and chipping mechanism but it is named due to high level of plastic flow forming lips around crater periphery. This fracturing mode was suggested by Hearley et al. [31-32] for both monolithic and thermally sprayed Stellite-6 alloy. After compression testing, fractured surface of Stellite-6/2 wt. % CNTs nanocomposites was studied in detail (Fig. 6). Addition of higher wt. % of CNTs does not have any impact in the change of composites fracture mode (from brittle to ductile). It remained brittle as it can be seen in fig. 6 that good number of lips had formed around crater periphery.
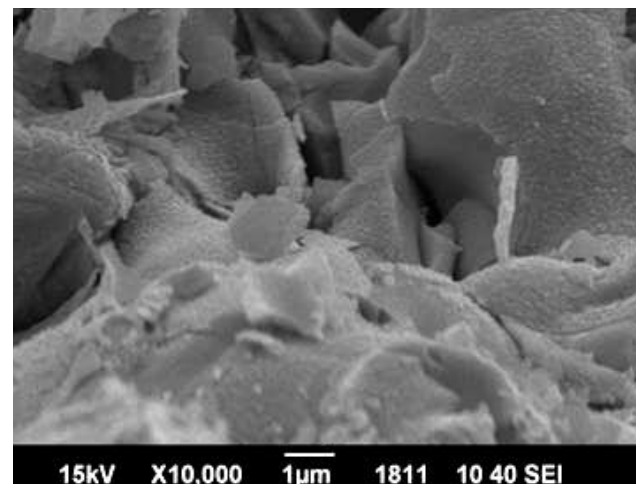

Fig. 6. Brittle behaviours of Stellite-6 /1.5 CNTs nanocomposites

4. Conclusions

Some interesting mechanical and fractured surface aspects of Stellite-6/CNTs nanocomposites were under consideration in this study. Varied wt. % of CNTs has quite noticeable impacts on hardness and compression behaviors of nanocomposites. Hardness values of monolithic Stellite-6 was in the range of 80 Hv and it increased with further addition of CNTs. The maximum hardness (185 Hv) value was for Stellite-6/1.5 wt. % CNTs nanocomposites. The increased hardness behaviors confirmed the effective reinforcing role of CNTs. As for as compression properties of nanocomposites are concerned (e.g. ultimate compressive strength and compression strain failure), these both increased in positive trends. Ultimate Compression Strength (UCS) of monolithic Stellite-6 was low (750 MPa) as compared to Stellite-6/2 wt. 5 CNTs nanocomposites (1100 MPa). Dislocations generation and more hurdles for dislocations to move always promote high stresses level to initiate plastic deformation in nanocomposites. Compression strain failures of Stellite-6/CNTs nanocomposites are also very good to report here. Monolithic Stellite-6 has lower strain failure % (22) as compared to Stellite-6/2 wt. % CNTs nanocomposites (31 %). There were no effects on the fracture behaviors of nanocomposites and it appeared in the same highly deformed mode (with the formation of lips around crater peripheries) as for monolithic Stellite-6.

References

[1] S. Iijima, Helical microtubules of graphitic, Nature **354** 56 (1991).

[2] N. Zhao, Q. Cui, C. He, C. Shi, J. Li, H. Li, X. Du, Materials Science and Engineering A **460**, 255 (2007).

[3] M. Caplovicova, L. Caplovic, D. Buc, P. Vinduska, J. Janık, Journal of Electrical Engineering **61**, 373 (2010).

[4] N. Zhao, C. He, Z. Jiang, J. Li, Y. Li, Materials Letters **60**, 159 (2006).

[5] J. P. S. Delmotte, A. Rubio, Carbon **40**, 1729 (2002).

[6] J. Salvetat, J. Bonard, N. Thomson, A. Kalik, L. Forro, W. Bnoit, Appl. Phys. A **69**, 255 (1999).

[7] X. Chen, R. Wang, J. Xu, D. Yu, Micron **35**, 455 (2004).

[8] Y. Murakami, Y. Miyauchi, S. Chiashi, S. Maruyama, Chemical Physics Letters **374**, 53 (2003).

[9] I. Stamatina, A. Morozana, A. Dumitrua, V. Ciupinab, G. Prodanb, J. Niewolskic, H. Figiel, Physica E **37**, 44 (2007).

[10] O. Guellati, S. Detriche, M. Guerioune, Z. Mkhalif, J. Delhalle, Int. J. Nanoelectronics and Materials **3**, 123 (2010).

[11] K. Raji, S. Thomas, C.B. Sobhan, Applied Surface Science **257**, 10562 (2011).

[12] E. Terrado, M. Redrado, E. Munoz, W. Maser, A.M. Benito, M.T. Martinez, Material Science and Engineering C **26**, 1185 (2006).

[13] M. Kumar, Y. Ando, Journal of Nanoscience and Nanotechnology **10**, 3739 (2010).

[14] S. Maruyama, R. Kojima, Y. Miyauchi, S. Chiashi, M. Kohno, Chemical Physics Letters **360**, 229 (2002).

[15] A. Okamoto, H. Shinohara, Carbon **43**, 431 (2005).

[16] G. O. Cervantez, G. R. Morales, J. O. Lopez, Microelectronics Journal **36**, 495 (2005).

[17] M. Wienecke, M. Bunescu, K. Deistung, P. Fedtke, E. Borchartd, Carbon **44**, 718 (2006).

[18] C. Pan, Y. Liu, F. Cao, J. Wanga, Y. Ren, Micron **35**, 461 (2004).

[19] G. Saeed, M. U. Farooq, Optoelectron. Adv. Mat. **7**(9-10), 707 (2013).

[20] Y. Birol, Materials Science and Engineering A**527**, 1938 (2010).

[21] H. Kashani, A. Amadeh, H.M. Ghasemi, Wear **262**, 800 (2007).

[22] Y. M. Feng, O. Laurie, M. J. Dyer, K. Moloni, Science **287**, 637 (2000).

[23] S. I. Cha, K. T. Kim, S. N, Arshad, Advanced Material **17**, 1377 (2005).

[24] S. R. Bakshi, D. Lahiri, A. Agarwal, International Materials Reviews **55**, 41 (2010).

[25] M. Burghard, K. Balasubramanian, Chemically Functionalized Carbon Nanotubes, Reviews **2**, 180 (2005).

[26] R. Casati, M. Vedani, Metal Matrix Composites Reinforced by Nano-Particles—A Review, Metals **4**, 65 (2014).

[27] S. F. Hassan, M. Gupta, Material Science and Technology **19**, 253 (2003).

[28] Z. Szaraz, Z. Trojanova, M. Cabbibo, E. Evangelista, Material Science and Engineering A **462**, 225 (2007).

[29] Q. B. Nguyen, M. Gupta, Composite Science and Technology **68**, 2185 (2008).

[30] Q. B. Nguyen, M. Gupta, Composite Material **43**, 5 (2009).

[31] H. S. Sidhu, B. S. Sidhu, S. Prakash, Surface & Coatings Technology **202**, 232 (2007).

[32] R. C. Shivamurthy, M. Kamaraj, R. Nagarajan, S. M. Shariff, G. Padmanabham, Metallurgical and Materials Transactions A **41**(A), 470 (2010).

_____

*Corresponding author: ghznfrsd190@hotmail.com